MOLECULAR AND CELLULAR BIOLOGY, July 2009, p. 3770–3782 Vol. 29, No. 13
0270-7306/09/$08.00+0 doi:10.1128/MCB.00204-09

Glycosyltransferase Function in Core 2-Type Protein O Glycosylation▽

Erica L. Stone,[1] Mohd Nazri Ismail,[2] Seung Ho Lee,[3] Ying Luu,[4] Kevin Ramirez,[1] Stuart M. Haslam,[2] Samuel B. Ho,[4] Anne Dell,[2] Minoru Fukuda,[3] and Jamey D. Marth[1]*

Howard Hughes Medical Institute and the Department of Cellular and Molecular Medicine, University of California, San Diego, La Jolla, California 92093[1]; Division of Molecular Biosciences, Faculty of Natural Sciences, Imperial College London, London SW7 2AZ, United Kingdom[2]; Burnham Institute for Medical Research, La Jolla, California 92037[3]; and Department of Medicine, VA San Diego Healthcare System and the University of California, San Diego, La Jolla, California 92161[4]

Received 13 February 2009/Accepted 25 March 2009

Three glycosyltransferases have been identified in mammals that can initiate core 2 protein O glycosylation. Core 2 O-glycans are abundant among glycoproteins but, to date, few functions for these structures have been identified. To investigate the biological roles of core 2 O-glycans, we produced and characterized mice deficient in one or more of the three known glycosyltransferases that generate core 2 O-glycans (C2GnT1, C2GnT2, and C2GnT3). A role for C2GnT1 in selectin ligand formation has been described. We now report that C2GnT2 deficiency impaired the mucosal barrier and increased susceptibility to colitis. C2GnT2 deficiency also reduced immunoglobulin abundance and resulted in the loss of all core 4 O-glycan biosynthetic activity. In contrast, the absence of C2GnT3 altered behavior linked to reduced thyroxine levels in circulation. Remarkably, elimination of all three C2GnTs was permissive of viability and fertility. Core 2 O-glycan structures were reduced among tissues from individual C2GnT deficiencies and completely absent from triply deficient mice. C2GnT deficiency also induced alterations in I-branching, core 1 O-glycan formation, and O mannosylation. Although the absence of C2GnT and C4GnT activities is tolerable in vivo, core 2 O glycosylation exerts a significant influence on O-glycan biosynthesis and is important in multiple physiological processes.

Protein O glycosylation is a posttranslational modification implicated in a wide range of physiological processes, including cell adhesion and trafficking, T-cell apoptosis, cell signaling, endocytosis and pathogen-host interaction (1, 6, 27, 30, 54, 61, 71). Core-type protein O glycosylation is initiated in the secretory pathway by the covalent addition of a *N*-acetylgalactosamine (GalNAc) to the hydroxyl group of serine or threonine residues by one of multiple polypeptide GalNAc transferases (ppGalNAcTs) (20, 44, 57, 58). After linkage of the GalNAc monosaccharide to serine or threonine, other glycosyltransferases sequentially and sometimes competitively elaborate the repertoire of O-glycan structures to include different core subtypes (31, 42, 48, 49).

The core 2 β1,6-*N*-acetylglucosaminyltransferases (C2GnTs) and the Core 2 O-glycans they generate are widely expressed among cells of mammalian species. The C2GnTs act after the core 1 β-1,3-galactosyltransferase adds a galactose in a β1,3-linkage to the GalNAc-Ser/Thr generating the initial core 1 O-glycan disaccharide structure (26). Then, one of the three C2GnTs (C2GnT1, C2GnT2, and C2GnT3) can add an *N*-acetylglucosamine (GlcNAc) in a β1,6-linkage to the GalNAc to initiate what is known as the core 2 O-glycan branch (Fig. 1a) (7, 50, 51, 69). In a distinct pathway, core 3 β-1,3-*N*-acetylglucosaminyltransferase (C3GnT) can add a GlcNAc to the unmodified GalNAc to generate a core 3 O-glycan (24). In this case, C2GnT2 can add a GlcNAc in β1,6-linkage to the GalNAc of the core 3 O-glycan disaccharide to initiate the formation of a core 4 O-glycan (Fig. 1b) (50, 69). In addition, both C2GnT2 and the I β-1,*6-N*-acetylglucosaminyltransferase (IGnT) are independently capable of forming branched polylactosamine structures (I-branches) from otherwise linear polylactosamine glycan chains (Fig. 1c) (69).

C2GnT1-deficient mice have been shown to have an unexpected phenotype first observed as leukocytosis reflecting neutrophilia (14). This appears to be due to a severe but selective defect in selectin ligand biosynthesis among myeloid cells, leading to decreased recruitment of neutrophils that attenuates inflammation and vascular disease pathogenesis (14, 64). C2GnT1-deficient mice also exhibit a partial reduction in L-selectin ligand biosynthesis on high endothelial venules, resulting in reduced B-cell homing and colonization of peripheral lymph nodes (18, 21). Furthermore, thymic progenitors from C2GnT1-deficient mice have a reduced ability to home to the thymus due to the loss of P-selectin ligands on these cells (46). However, as of yet, C2GnT2 and C2GnT3 have not been similarly investigated, and their biological functions remain to be elucidated. To further investigate why multiple glycosyltransferases capable of core 2 O-glycan formation have been conserved, we have generated mice singly and multiply deficient in the three known C2GnTs and characterized the resulting physiology and alterations to the glycome.

MATERIALS AND METHODS

Mice. Genomic clones isolated from the 129/SvJ mouse strain were used to construct targeting vectors for *Gcnt3*, encoding C2GnT2, and *Gcnt4*, encoding C2GnT3. To generate individual targeting vectors for each gene, the genomic clones and the pflox vector were digested with the appropriate restriction enzymes as indicated (Fig. 2). Each genomic clone was then ligated into the pflox vector to generate the targeting vector for each gene. The targeting vectors were then individually electroporated into R1 embryonic stem (ES) cells (39). Homologous recombination between the targeting vector and genomic DNA re-

* Corresponding author. Mailing address: UCSD, 9500 Gilman Drive 0625, La Jolla, CA 92093. Phone: (858) 534-6526. Fax: (858) 534-6724. E-mail: jmarth@me.com.

▽ Published ahead of print on 6 April 2009.

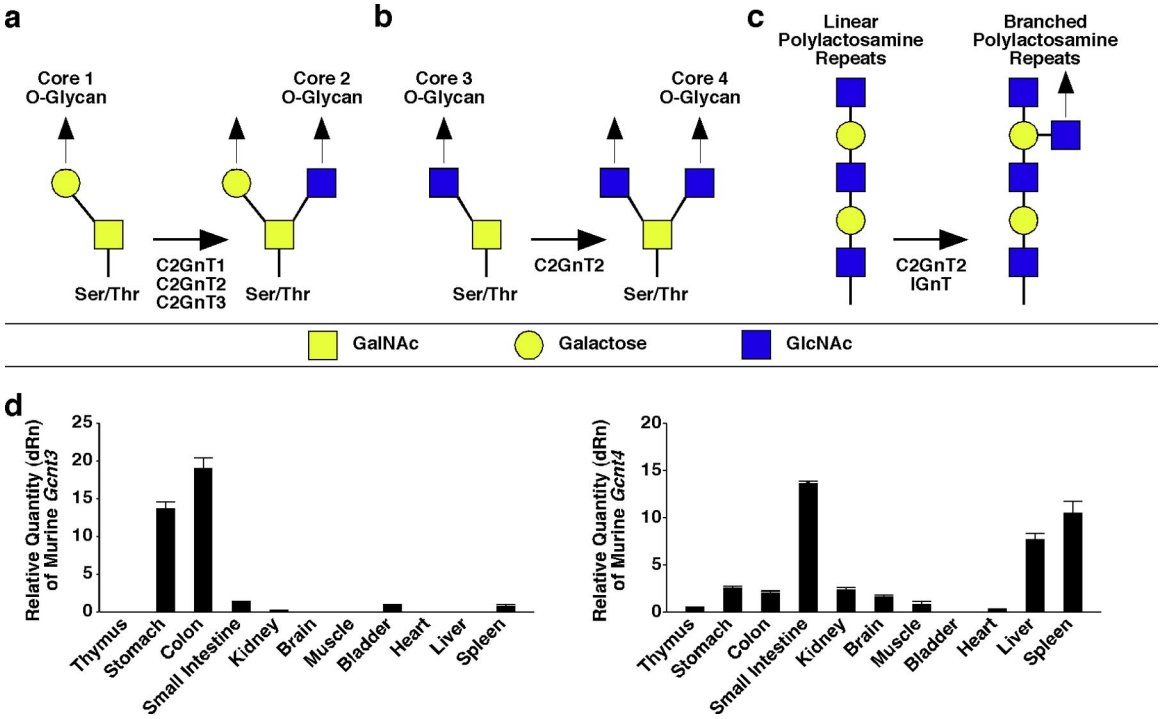

FIG. 1. Activity and expression of C2GnTs. (a to c) Monosaccharides are depicted as geometric shapes, with GalNAc as a yellow square, galactose as a yellow circle, and GlcNAc as a blue square. In addition, the vertical arrows indicate that each branch can be further elaborated by additional saccharide linkages. (a) Biantennary core 2 O-glycans are generated when any of the three C2GnTs acts on the core 1 O-glycan disaccharide. (b) C2GnT2 can generate core 4 O-glycans from core 3 O-glycans by adding a GlcNAc to the initiating GalNAc. (c) C2GnT2, in addition to IGnT, also has the ability to generate branched polylactosamine repeats from linear polylactosamine repeats. The figure depicts distal I-branching as the GlcNAc is transferred to the predistal galactose, the preferential I-branching activity of C2GnT2. However, IGnT preferentially has central I-branching activity that adds GlcNAc on the internal galactose in Galβ1→4GlcNAcβ1→3Gal-R (69). (d) RNA expression of murine *Gcnt3* (left panel) and *Gcnt4* (right panel), which code for C2GnT2 and C2GnT3, respectively, as determined by qPCR. The data on single animals are graphed relative to testes expression. All values are means ± the standard errors of the mean (SEM).

sulted in F[tk-neo] alleles. G418 (to select for *neo* gene expression) was used to select for cells in which the targeting vectors had integrated. A Cre recombinase-expressing plasmid was electroporated into these cells. Ganciclovir was used to select for colonies in which thymidine kinase (tk) was deleted by Cre recombinase activity. Southern blotting of genomic DNA confirmed the expected allelic structures were present. Individual chimeric mice were obtained from C57BL/6NHsd blastocytes injected separately with ES cells containing the alleles in which the single coding exon of interest was flanked by loxP sites. Mice carrying these alleles, $Gcnt3^{F}$ or $Gcnt4^{F}$, in the germ line were crossed with female ZP3-Cre mice to generate separate mice with systematic deletions, i.e., $Gcnt3^{\Delta/\Delta}$ or $Gcnt4^{\Delta/\Delta}$ mice. Experimental mice were from a mixed background of 129Sv/J and C57BL/6NHsd mice; for this reason, littermate control mice were used whenever possible.

Crossing of singly deficient strains generated mice deficient in multiple C2GnTs. C2GnT1-deficient mice, which have been previously described (14), were crossed to C2GnT3-deficient mice to generate mice heterozygous for both alleles. These doubly heterozygous mice were bred to each other to generate mice doubly deficient for C2GnT1 and C2GnT3 (T1/T3). T1/T3 mice were then bred to C2GnT2-deficient mice to generate mice heterozygous for all three genes encoding C2GnTs. Triply heterozygous mice were bred together to generate offspring doubly deficient for C2GnT1 and C2GnT2 (T1/T2) and doubly deficient for C2GnT2 and C2GnT3 (T2/T3), as well as mice deficient for all three C2GnTs (T1/T2/T3). Some T1/T2/T3 mice were used in additional breedings to generate experimental mice. Animal studies were performed in accordance with the Institution Animal Care and Use Committee of the University of California, San Diego.

qPCR. RNA was obtained from wild-type C57BL/6NHsd mice. Tissues were harvested and stored at −80°C. To isolate the RNA, the tissue sample was placed in TRI-Reagent (Sigma, St. Louis, MO) and homogenized. After homogenization chloroform (Sigma) was added for extraction. RNA was pelleted by using isopropanol (Sigma) and cleaned using 70% ethanol. RNA was dissolved in H_2O and treated with Turbo DNA-free (Ambion, Austin, TX) to remove DNA. RNA was run on an agarose-formaldehyde gel to determine quality and stored at −80°C. RNA was quantified using an optical density at 260 nm and diluted to 0.5 μg/μl. Quantitative PCR (qPCR) was done as previously described with slight modifications (36). cDNA was generated by using 1 μg of RNA and Superscript III First Strand (Invitrogen, Carlsbad, CA). cDNA product was diluted 1/10 in H_2O, and 1 μl of diluted cDNA plus 0.5 μM of each primer was used with Brilliant SYBR green (Stratagene, Cedar Creek, TX) for the qPCR reaction. AGGCTCCTCTTCCCTCAAAG was used for the *Gcnt4* forward primer, and ACATCACCGTCCTCCAAGTC was used as the *Gcnt4* reverse primer. The results were standardized by using β-actin.

Selectin ligand expression. Selectin ligand expression was analyzed as previously described with slight modifications (14, 59). Chimeras consisting of the lectin domains of mouse E- or P-selectin and the Fc portion of human immunoglobulin G (IgG; R&D Systems, Minneapolis, MN) were bound to fluorescein isothiocyanate (FITC)-conjugated anti-human IgG antibody (Fc specific; Sigma) in binding medium consisting of Dulbecco modified Eagle medium (Gibco) plus 2% IgG-free bovine serum albumin (BSA; Jackson Immunoresearch, West Grove, PA) plus 2 mM $CaCl_2$ or 5 mM EDTA and placed in the dark at 4°C for 30 min. White blood cells were washed with binding medium and then stained with selectin-Fc chimeras prebound to anti-human Fc-FITC. Selectin chimera binding to white blood cells was determined by flow cytometry using a FACSCalibur (BD Biosciences, San Jose, CA).

To activate T cells, splenocytes were cultured in RPMI media plus 10% bovine serum in the presence of plate-bound anti-CD3 (BD Biosciences) and 20 ng of interleukin-2 (R&D Systems)/ml for 48 h. At the indicated time points, cells were suspended in binding medium, and the expression of activation markers or selectin ligands was determined by flow cytometry.

Hematology. Hematological parameters were determined utilizing a Hemavet 850FS (Drew Scientific, Wayne, PA) as previously described (59).

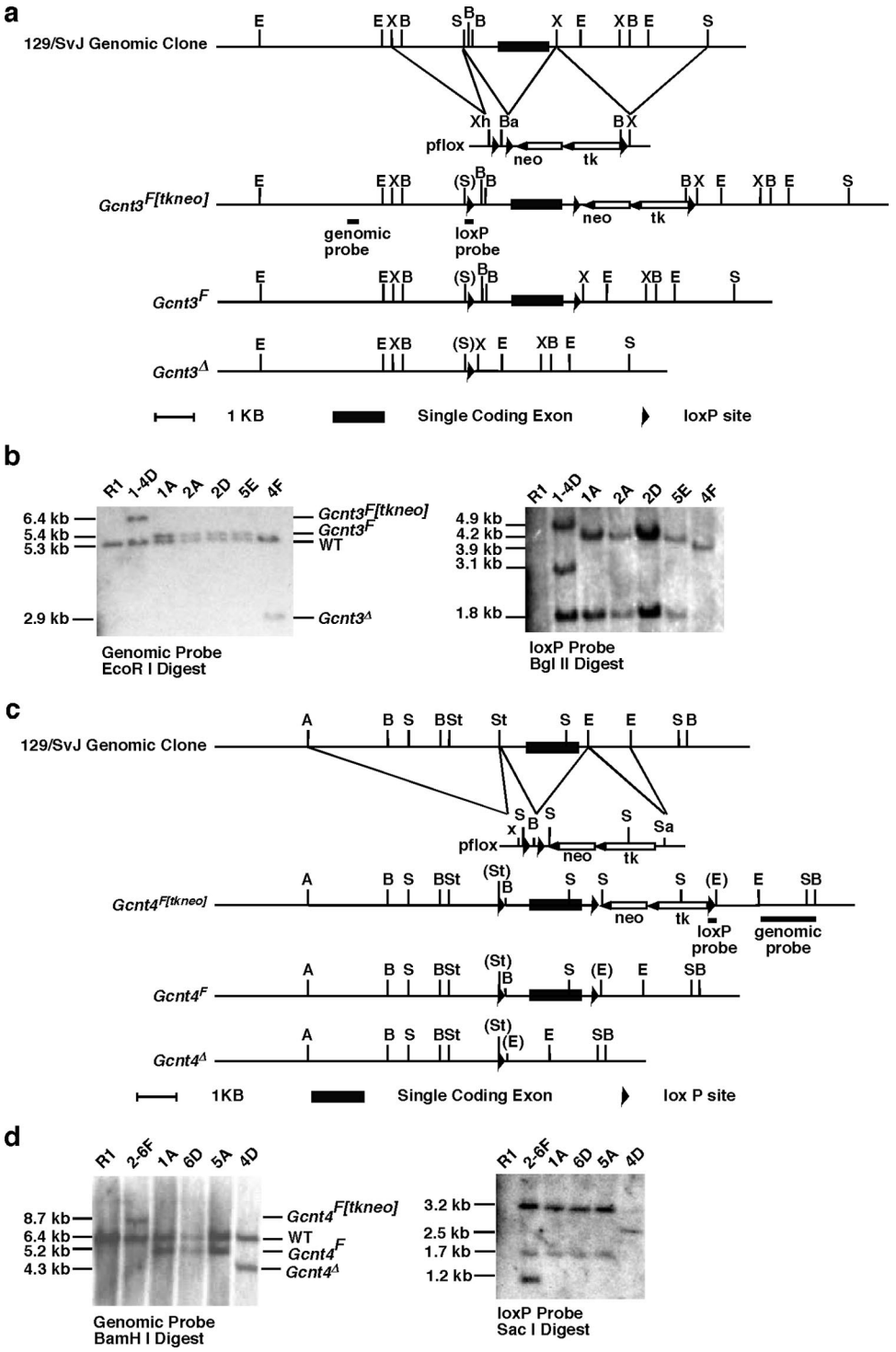

FIG. 2. Generation of mice singly deficient for C2GnT2 or C2GnT3. (a) *Gcnt3* genomic clone from 129/SvJ mouse strain was used to generate a targeting construct using the pflox vector as indicated. B, BglII; Ba, BamHI; E, EcoRI; S, SpeI; X, XbaI; Xh, XhoI. (b) Southern blotting of genomic DNA confirms the *Gcnt3* allele structure present in ES cells using the genomic probe (top). Southern blotting with a loxP probe detects the location and number of loxP sites (bottom). (c) The targeting of the single coding exon of *Gcnt4* using the pflox vector is depicted. A, AgeI; B, BamHI; E, EcoRV; S, SacI; Sa, SalI; St, StuI; X, XhoI. (d) Southern blots of genomic DNA with the genomic probe (top) or loxP probe (bottom) indicate the structure of the *Gcnt4* alleles present. WT, wild type.

In vivo mucosal permeability assay. Mucosal barrier function was determined as previously described (17). Dextran-FITC (Sigma) was administered via oral gavage (600 mg/kg), and blood was collected into Microtainer serum separator tubes (Becton Dickinson, Franklin Lakes, NJ) by retro-orbital bleeds at 4 h. Blood was spun down in a tabletop centrifuge at 16.1 × *g* for 3 min to separate sera. The amount of FITC in each sample was measured in duplicate by using Spectra Max Gemini EM fluorescent plate reader (Molecular Devices) at 490 and 530 nm for the excitation and emission wavelengths, respectively.

DSS-induced colitis. Mice were administered drinking water containing 5% dextran sodium sulfate (DSS; molecular weight, 40,000 to 50,000; USB Corp., Cleveland, OH) ad libitum and then returned to normal drinking water without DSS. DSS was administered for 5 or 6 days. The presence of occult or overt blood in the stool, stool consistency, weight, and the activity level of each mouse were determined daily throughout the experiment and used to calculate disease activity index as previously described (22). Mice surviving to the end of the experiment were then sacrificed, and colons were fixed in 10% buffered formalin for histological analyses. The amount of 5% DSS ingested was monitored daily and did not differ between groups. Mice that did not drink enough to surpass a DSS-load of 30 mg/day were excluded from the study. Colon sections were stained with hematoxylin and eosin (H&E). The severity of mucosal injury was graded similarly to methods described previously (38, 40). Briefly, H&E-stained sections were read in a blinded manner to determine length of colon ulceration and the crypt damage score. The injury scale was graded from 0 to III as follows: grade 0, normal; grade I, distortion and/or destruction of the bottom third of glands; grade II, erosions/destruction of all glands or the bottom two-thirds of glands and inflammatory infiltrate with preserved surface epithelium; and grade III, loss of entire glands and surface epithelium. The results are reported as the total length of complete ulceration (grade III damage) and the total crypt damage score as described previously (22).

Mucosal protein assays. A solution containing proteins from the mucosal layer was produced as described earlier (13) with slight modification. Feces were collected in a clean, empty cage for 1 h. The feces were weighed, diluted 20-fold weight to volume in phosphate-buffered saline (PBS), and vortexed to make a fecal solution.

Relative Muc2 levels were determined by enzyme-linked immunosorbent assay (ELISA). Maxisorp 96-well plates (Nunc, Rochester, NY) were coated overnight at 4°C with fecal solution diluted 10-fold further with PBS. The plates were washed with PBS, blocked with PBS plus 2% IgG-free bovine serum albumin (BSA; Jackson Immunoresearch) for 1 h at 22°C, and then washed with PBS plus 0.05% Tween 20 (PBST; Fisher Scientific, Pittsburg, PA). Antibody to Muc2 antigen H-300 (Santa Cruz Biotechnology, Santa Cruz, CA) diluted to 0.2 μg/ml in PBS plus 2% BSA was then allowed to bind overnight at 4°C. The plates were then washed and coated with the secondary anti-rabbit antibody conjugated to horseradish peroxidase (Vector Laboratories, Burlingame, CA) diluted 1/1,000 in PBS plus 2% BSA. Tetramethylbenzidine (Sigma) was used as a substrate, and the plates were analyzed at 650 nm by using a VersaMax plate reader (Molecular Devices, Sunnyvale, CA).

Immunoglobulin analyses. Flat-bottom Maxisorp 96-well plates were coated with 5 μg of anti-mouse isotype-specific antibodies (IgM, IgG1, IgG2a, IgG2b, IgG3, and IgA; BD Biosciences)/ml in PBS overnight at 4°C. Plates were blocked with 2% BSA. Serum samples were diluted 1/2,000 (for IgG1, IgG2a, and IgA) or 1/10,000 (for IgG3, IgM, and IgG2b) in PBS plus 2% BSA and then incubated for 2 h at 22°C. Fecal solutions were diluted 1/100 in PBS plus 2% BSA. Plates were washed with PBST. Alkaline phosphatase (AP)-conjugated antibodies to mouse IgG1, IgG2a, IgG2b, and IgG3 (BD Biosciences) were diluted 1/500 in PBS plus 2% BSA. AP-conjugated antibodies to mouse IgM (1/4,000) and IgA (1/1,000) were purchased from Sigma. Plates were incubated with these secondary antibodies for 1 h at 22°C and washed with PBST, and then the AP substrate *para*-nitrophenyl phosphate (Sigma) was added. Signals were determined at 405 nm on a VersaMax plate reader.

Behavioral testing. Behavioral screening included gross physical assessment, analysis of sensorimotor reflexes, and the following assays: acoustic startle, prepulse inhibition, hot plate, tail flick, conditioned fear, initiation of movement, rotarod, wire hang, grip strength, cage-top hang test, and pole test. These tests were accomplished as previously reported (3, 28). In the tube test for social dominance, mice of different genotypes are put into opposite ends of a 30-cm-long tube (29). The mouse that stays in the tube and causes the other to back out is considered dominant and has "won" the challenge. If neither mouse backed out of the tube within 60 s, the challenge was deemed a "tie." Each mouse was challenged three times against three different mice, including littermates of the opposite genotype.

Determination of thyroid hormone levels. T4 levels were determined by T4 enzyme immunoassays (Monobind, Inc., Lake Forest, CA). Thyroid-stimulating hormone (TSH) levels were determined by a two-site chemiluminometric assay at the Hillcrest Medical Center of UC San Diego Medical Center.

Thyroid powder supplemented diet. Chow was supplemented with 0.025% porcine thyroid powder (Sigma) as previously described (34) with minor modifications. The Purina 5053 base diet supplemented with 0.025% porcine thyroid powder was used (Purina, Richmond, IN). Thyroid powder-supplemented chow was fed to wild-type and C2GnT3-deficient mice for 2 weeks in a conventional vivarium. Mice were analyzed by the tube test for social dominance prior to and after diet supplementation. In addition, sera were collected at both time points following the tube test for social dominance. Sera were stored at −20°C until used to determine T4 levels.

TRH stimulation assay. Mice were stimulated with thyrotropin-releasing hormone (TRH) as previously described (67) with minor modifications. Blood was obtained at time zero, and then mice were immediately given, by intraperitoneal injection, 5 μg of TRH (Sigma)/kg dissolved in 100 μl of PBS. Blood was then collected into serum separator tubes (Becton Dickinson) at 1 or 2 h and centrifuged at 16.1 × *g* for 3 min to separate sera. Sera were stored in fresh microfuge tubes at −20°C until analyzed.

T4 half-life assay. NHS-LC-biotin (10 mg/kg of body weight; Pierce, Rockland, IL) was injected intravenously into mice to biotinylate circulating proteins as similarly described (19). Mice were then bled at time zero. Blood was collected at additional time points in serum separator tubes. Sera were stored at −20°C until assayed. Glycine was added to sera to quench any additional NHS activity. Biotinylated T4 remaining was determined by ELISA. A flat-bottom Maxisorp plate was coated overnight at 4°C with anti-T4 antibody (Santa Cruz Biotechnology) diluted 1/1,000 in PBS. The plates were washed with PBS and then blocked overnight at 4°C with PBS plus 2% BSA. Serum samples were incubated on the blocked plates for 1 h at 22°C, and the plates were then washed with PBST. Streptavidin-horseradish peroxidase (BD Biosciences) diluted 1/5,000 in PBS plus 2% BSA was allowed to bind for 45 min at 22°C. The plates were washed again, tetramethylbenzidine substrate was added, and the plates were read at 650 nm by using a VersaMax plate reader.

Enzyme activity assays. Tissues from freshly sacrificed mice were immediately frozen using dry ice and stored at −80°C until used. C2GnT and C4GnT activities from tissue lysates were determined as previously described (69).

Sample preparation for mass spectrometric (MS) analysis. Murine tissues were prepared for glycomic screening according to methodology described previously (56). Briefly, murine tissues were homogenized with Tris buffer and sequentially digested with trypsin (Sigma-Aldrich, Dorset, United Kingdom) and PNGase F (Roche, West Sussex, United Kingdom). N-glycans were separated from peptides and/or glycopeptides on Sep-Pak cartridges (Waters, Hertfordshire, United Kingdom), and O-glycans were released from the latter by reductive elimination using KBH_4 in KOH. To optimize O-glycan extraction from mucinous tissues, especially the stomach, the following modifications were applied to the previous procedure. Stomach samples were homogenized with water, and then glycolipids were extracted with methanol and chloroform. After trypsin digestion, O-glycans were released from the glycopeptide/peptide pool without N-glycan removal. Although trace amounts of N-glycans might be released together with O-glycans, this strategy permits an improved recovery of O-glycans.

After purification on Dowex columns (Sigma-Aldrich), the O-glycan samples were permethylated and then further purified with Sep-Pak cartridges. O-glycans were eluted in aqueous acetonitrile fractions and then lyophilized. Glycans are normally eluted in the 35 and 50% acetonitrile fractions; therefore, only these fractions were subjected to MS analysis. All murine tissues were analyzed in duplicates or triplicates.

MS data acquisition. Permethylated samples were dissolved in 10 μl of methanol. Then, 1 μl of dissolved sample was premixed with 1 μl of matrix (20 mg of 2,5-dihydroxybenzoic acid/ml in 70% [vol/vol] aqueous methanol) and spotted onto a target plate. Matrix-assisted laser desorption ionization (MALDI) MS and tandem MS (MS/MS) data were acquired on a 4800 MALDI-TOF/TOF mass spectrometer (Applied Biosystems) in the reflectron mode. The potential difference between the source acceleration voltage and the collision cell was set to 1 kV, and argon was used as the collision gas. The 4700 Calmix calibration standard kit (Applied Biosystems) was used as the external calibrant for the MS mode, and [Glu1]fibrinopeptide B human (Sigma-Aldrich) was used as an external calibrant for the MS/MS mode.

Comparison of the relative abundance of O-glycans between C2GnT2-deficient, C2GnT3-deficient, and T1/T2/T3 mice with wild-type mice of various tissues was done by comparing the peak heights of molecular ions of similar masses and by comparing the total ion counts of the different classes of glycans.

Statistical analyses. The significance in the tube test for social dominance was determined by the chi-square test. For all other experiments, the Student *t* test was used to determine statistical significance.

RESULTS

Expression of murine *Gcnt3* and *Gcnt4* RNA. Glycosyltransferases that generate core 2 O-glycans are encoded by separate genes each with a single coding exon in the murine and human genomes. C2GnT1 is encoded by *Gcnt1*, C2GnT2 is encoded

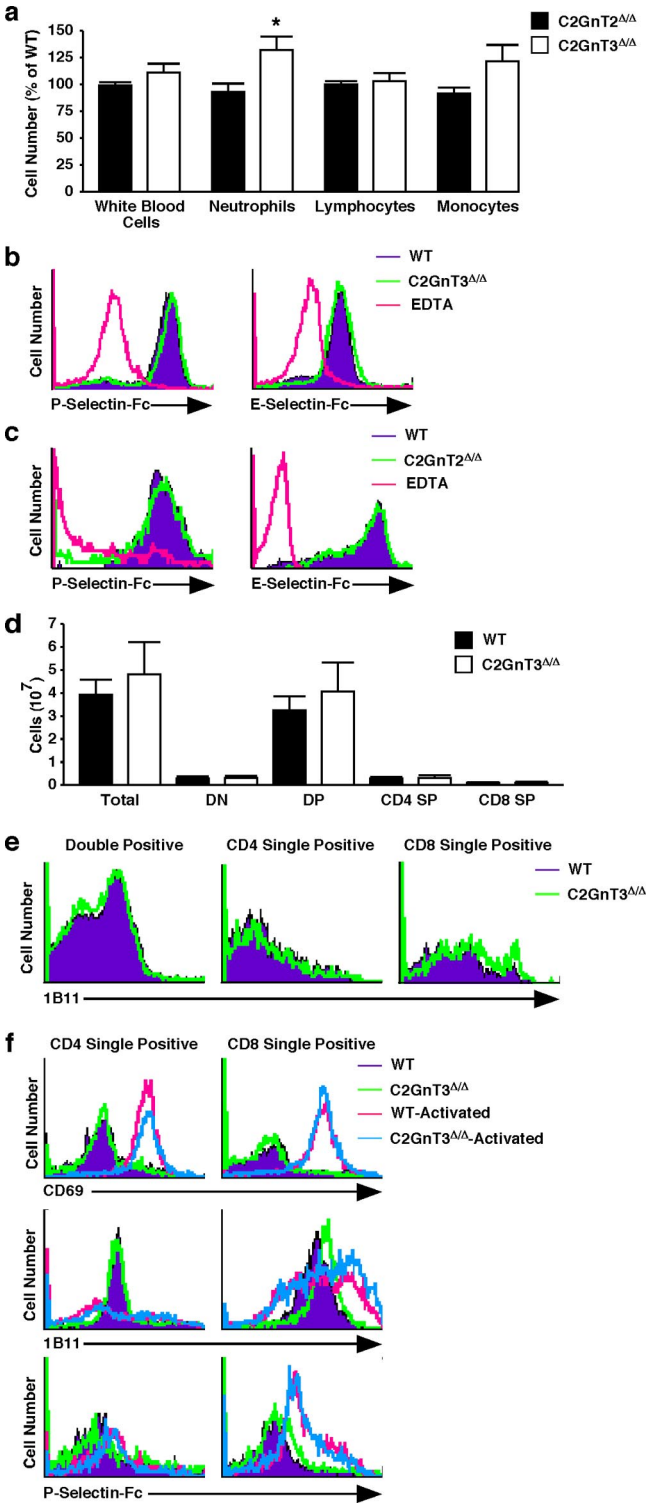

FIG. 3. Selectin ligand expression on neutrophils and T cells from C2GnT-deficient mice. (a) Hematological levels in mice singly deficient for C2GnT2 or C2GnT3 relative to wild-type levels are graphed. (b and c) Histograms depict the expression of ligands for P- and E-selectins on neutrophils from mice singly deficient for C2GnT3 (b) or C2GnT2 (c). Addition of EDTA controls for binding of C-type lectins. (d) The number of thymocytes of each cell type in wild-type and C2GnT3-deficient mice is graphed (DN, $CD4^-$ $CD8^-$ cells; DP, $CD4^+$ $CD8^+$ cells; SP, $CD4^+$ or $CD8^+$ cells). (e) Expression of the 1B11 antigen on thymocyte subpopulations. (f) Histograms indicate the level of expression of activation markers and selectin ligands on activated wild-type and C2GnT3-deficient T cells. All values are means ± the SEM (*, $P < 0.05$). WT, wild type.

by *Gcnt3*, and C2GnT3 is encoded by *Gcnt4*. The numbering of the genes and the enzymes differ because the genes were named based on β1,6-GlcNAc transferase activity and the enzymes were named based on Core 2 activity. *Gcnt2* encodes IGnT, which has β-1,6-GlcNAc transferase activity but is not able to generate core 2 O-glycans, since it is not able to act upon the core 1 O-glycan as a substrate (32).

Analysis of relative expression of *Gcnt3* in adult wild-type C57BL/6Nhsd mouse tissues by qPCR revealed that *Gcnt3* has high relative expression in the gastrointestinal tract, similar to the previously determined expression pattern of human *GCNT3* (69). In contrast to the expression of human *GCNT4* (51), relatively low levels of the mouse orthologue *Gcnt4* were found in the thymus. Our studies revealed the highest levels of expression of murine *Gcnt4* in the small intestine, liver, and spleen (Fig. 1d).

Germ line deletion of *Gcnt3* and *Gcnt4*. *Gcnt3* and *Gcnt4* were targeted separately for deletion from the mouse germ line. *Gcnt3* was targeted in ES cells using Cre-loxP conditional mutagenesis focused on the single coding exon of *Gcnt3* (Fig. 2a). ES cells in which loxP sites flanked the single coding exon of Gcnt3 were utilized to generate chimeric mice (Fig. 2b). $Gcnt3^F$ mice were bred to mice expressing Cre recombinase, under the control of the Zp3 promoter (52), to generate mice with a systematic deletion of *Gcnt3* ($Gcnt3^\Delta$). C2GnT2-deficient mice ($Gcnt3^{\Delta/\Delta}$) were viable, born at normal Mendelian ratios, and both genders were fertile.

The single coding exon of *Gcnt4* was similarly targeted using the Cre-loxP mutagenesis approach (Fig. 2c). Chimeric mice were generated with ES cells that carried the $Gcnt4^F$ allele (Fig. 2d). Breeding to Zp3-Cre mice was again utilized to produce offspring carrying the $Gcnt4^\Delta$ allele in the germ line (Fig. 2d). Both genders of mice homozygous for the $Gcnt4^\Delta$ allele were also born at expected Mendelian ratios without overt developmental abnormalities and exhibited normal fecundity as adults.

Hematology and selectin ligand biosynthesis in mice lacking either C2GnT2 or C2GnT3. Since the selectin ligand biosynthesis defect in C2GnT1-deficient mice is incomplete and since there is precedence for collaboration among glycosyltransferases in the biosynthesis of selectin ligands (35, 45), we analyzed mice lacking either C2GnT2 or C2GnT3 for signs of a selectin ligand defect. Hematological analyses revealed that C2GnT3-deficient mice ($Gcnt4^{\Delta/\Delta}$), but not C2GnT2-deficient mice, exhibited slight, but significant neutrophilia. No other alterations in hematological profiles were evident in mice singly deficient for C2GnT2 or C2GnT3 (Fig. 3a). In addition, no overt differences were observed in the cellularity of various immune tissues, including in the peripheral lymph nodes, or in the expression of various markers on immune cells, including B220 (data not shown). To determine whether the neutrophilia exhibited by C2GnT3-deficient mice is a result of reduced selectin ligand biosynthesis in the absence of C2GnT3, selectin ligand expression on neutrophils from C2GnT3-deficient mice

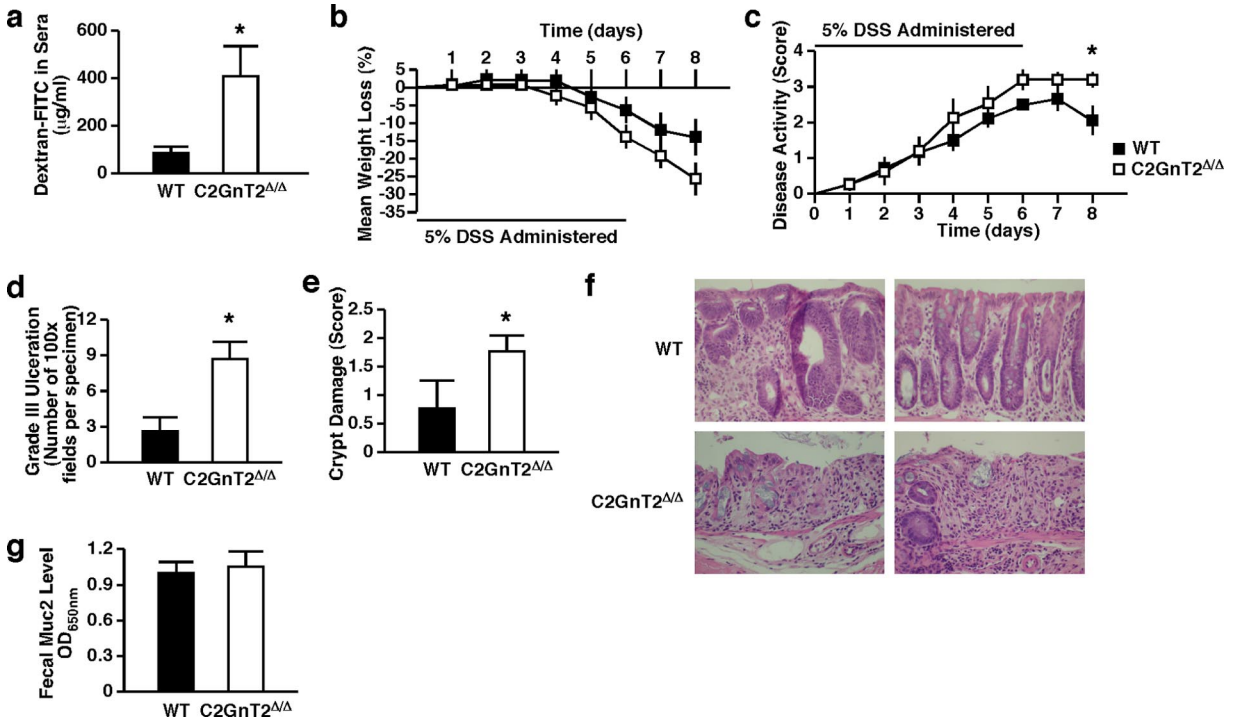

FIG. 4. Barrier function and colitis in C2GnT2-deficient mice. (a) The amount of dextran-FITC in sera 4 h after administration by gavage is graphed. The data shown are from a minimum of six mice per genotype. (b) Graph shows the average percent weight change compared to $t = 0$ of wild-type (■) and C2GnT2-deficient (□) mice during and after treatment with 5% DSS until the onset of mortality. The horizontal line represents the time of the DSS treatment. DSS was given to six mice of each genotype. (c) Disease activity index of wild-type and C2GnT2-deficient mice treated with 5% DSS is graphed. (d) The length of grade III damage (total ulceration with loss of glands and surface epithelium) in colon sections from of DSS-treated wild-type and C2GnT2-deficient mice is shown. (e) The average crypt damage score is graphed. (f) Representative H&E-stained colon sections from DSS-treated wild-type mice (illustrating grade II and grade I crypt damage) and C2GnT2-deficient mice (illustrating grade III crypt damage or total ulceration). (g) Relative mucosal Muc2 levels from untreated wild-type and C2GnT2-deficient mice is graphed. All values are means ± the SEM. The SEM is represented by capped and uncapped vertical lines ($P < 0.05$). WT, wild type.

was analyzed. Using flow cytometric measurements, neutrophils from these mice expressed unaltered P- and E-selectin ligands (Fig. 3b). C2GnT2-deficient neutrophils also normally expressed ligands for P- and E-selectins (Fig. 3c). In addition, the homeostasis of thymocytes within C2GnT3-deficient mice was unaltered (Fig. 3d). C2GnT3-deficient thymocytes also exhibited normal expression of cell surface markers including 1B11, which is partly dependent upon core 2 O glycosylation (8) (Fig. 3e). Since selectin ligand expression is upregulated by activated T cells and C2GnT3 is expressed in activated T cells (36), we analyzed the expression of selectin ligands on activated C2GnT3-deficient T cells. Upon stimulation with plate-bound anti-CD3 antibody in the presence of IL-2, C2GnT3-deficient T cells upregulated activation markers, including CD69 and 1B11, similarly to activated wild-type T cells (Fig. 3f). Selectin ligand expression, as determined by cytometry, was also unaltered among these activated T cells, revealing that C2GnT3 is not required for upregulation of selectin ligands under these conditions.

C2GnT2 deficiency impairs mucosal barrier function and increases the pathogenesis of experimental colitis. Since *Gcnt3* is relatively highly expressed in tissues with high epithelial cell content, we suspected that the gastrointestinal tract might be affected in C2GnT2 deficiency. In fact, C2GnT2-deficient mice, but not C2GnT3-deficient mice, were found to have increased mucosal permeability, indicating a defect in the mucosal barrier (Fig. 4a and data not shown). To test the ability of the gastrointestinal tract of C2GnT2-deficient mice to protect from chemically induced colitis, we used DSS to experimentally induce disease (22). There was a trend toward increased weight loss in C2GnT2-deficient mice treated with DSS (Fig. 4b). Also, on at least 1 day during each separate experiment the disease activity score for C2GnT2-deficient mice was significantly worse than for similarly treated wild-type counterparts (Fig. 4c). At the end of the experiment, H&E-stained colon sections were used to determine the length and grade of ulceration in these tissues. DSS-treated C2GnT2-deficient mice exhibited significantly more colon damage with increased ulceration and increased damage to the crypts in the colon (Fig. 4d, e, and f).

Mucins, glycoproteins that derive a majority of their molecular mass from O-glycans, have been implicated in mucosal barrier function and protection from DSS-induced colitis (47, 60). However, the expression of Muc2, the major secretory mucin in the colon, is not reduced among mice deficient in C2GnT2 (Fig. 4g).

Immunoglobulin deficiencies in the absence of C2GnT2. Levels of IgG1, IgG2a, and IgG2b were significantly reduced in the serum of C2GnT2-deficient mice (Fig. 5a). There is also a trend toward decreased serum levels of IgG3 and IgA. In

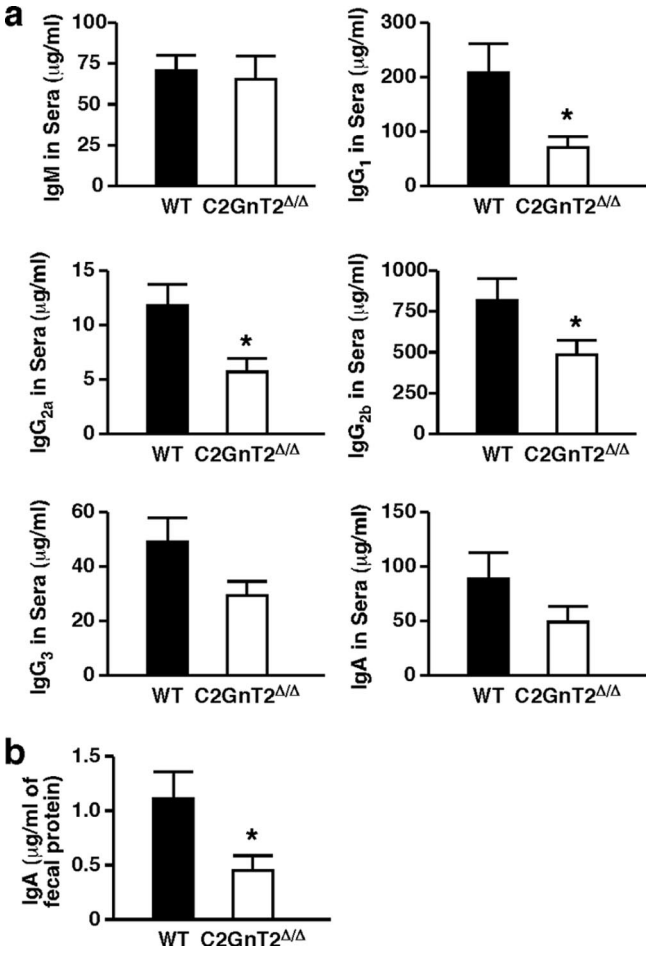

FIG. 5. Circulating and mucosal immunoglobulins in wild-type and C2GnT2-deficient mice. (a) The circulating levels of IgM, IgG1, IgG2a, IgG2b, IgG3, and IgA isotypes in wild-type and C2GnT2-deficient mice are graphed. The data shown are pooled from two separate experiments, each of at least five mice of each genotype per an experiment. (b) The mean mucosal IgA levels in wild-type and C2GnT2-deficient mice fecal samples are graphed. All values are means ± the SEM (*, $P < 0.05$). WT, wild type.

contrast to circulating IgA, mucosal IgA abundance was significantly decreased in C2GnT2-deficient mice (Fig. 5b). Altered mucosal immune homeostasis, including the absence of mucosal immunoglobulins, has previously been associated with susceptibility to DSS-induced colitis (9, 37). Absence of C2GnT2 results in a defect in the immune system, characterized by a reduction in immunoglobulin levels that may be associated with an increase in disease susceptibility.

C2GnT3-deficient mice exhibit a behavioral abnormality linked to reduced thyroxine levels. Increased fighting was observed between male mice in litters containing at least one C2GnT3-deficient animal, but not among litters that included C2GnT2-deficient mice. The behavior of male mice lacking C2GnT3 was further analyzed. C2GnT3-deficient male mice exhibited a significant increase in social dominance compared to wild-type male littermates (Fig. 6a). This assay is often used as a measure of aggression (10). Hypothyroidism is one cause of aggression in mammals, including dogs and horses (4, 12, 15, 62). Further analyses revealed that C2GnT3-deficient mice had a slight but significant decrease in circulating thyroxine (T4) levels (Fig. 6b). To determine whether the altered behavior observed in C2GnT3 deficiency was a result of insufficient T4 abundance, we fed C2GnT3-deficient mice and wild-type littermates chow supplemented with 0.025% porcine thyroid powder (34). Wild-type and C2GnT3-deficient mice fed thyroid-powder supplemented chow achieved similar circulating T4 levels (Fig. 6c). When these mice were retested in the social dominance assay, no difference between C2GnT3-deficient and wild-type mice was observed (Fig. 6d). This finding indicates that the altered behavior observed in C2GnT3-deficient mice is likely due to reduced T4 levels in circulation.

The thyroid is stimulated to release T4 in response to the secretion of TSH from the pituitary. Thus, we investigated the abundance of TSH in circulation in C2GnT3-deficient mice. No difference was observed in circulating TSH abundance (Fig. 6e). Reduced levels of circulating T4, in the presence of normal levels of TSH, suggests secondary hypothyroidism because thyroid hormone regulation involves a negative-feedback loop in which T4 feeds back to the pituitary to reduce TSH secretion (11, 16). Secondary hypothyroidism can be tested by stimulation with TRH, the hormone secreted from the hypothalamus that stimulates the pituitary to release TSH (41, 67). No differences were present in the levels of T4 secreted in response to TRH stimulation among wild-type and C2GnT3-deficient mice (Fig. 6f). This suggests that the slight reduction in T4 levels may not be sufficient to increase TSH levels via the negative-feedback loop.

The mild hypothyroidism in C2GnT3-deficient mice may not be a result of secondary hypothyroidism despite normal levels of TSH. To determine whether T4 levels are reduced due to decreased half-life in circulation, we compared the in vivo half-life of T4 in wild-type and C2GnT3-deficient mice. No difference in T4 half-life in wild-type and C2GnT3-deficient mice was detected (Fig. 6g).

Mice deficient for all three C2GnTs are viable. The extent to which the three known glycosyltransferases with C2GnT activity can biologically compensate for each other is unknown; thus, we chose to generate mice deficient for multiple C2GnTs. Since these three *Gcnt* genes reside on different chromosomes, we accomplished this by crossing the singly deficient states to each other. All three possible C2GnT doubly deficient combinations (T1/T2, T1/T3, and T2/T3) were generated, and these animals were born without overt abnormalities and appeared normal. From these parental sources, offspring should theoretically include triple-null littermates (T1/T2/T3). Remarkably, mice deficient in all three C2GnTs were born viable and appeared to develop normally to adults. In addition, both male and female T1/T2/T3 mice were fertile (data not shown).

C2GnT and C4GnT activity in C2GnT-deficient mice. C2GnT2 and C2GnT4 enzymatic activity levels were determined among tissue lysates from animals bearing single and multiple C2GnT deficiencies. C2GnT2-deficient mouse colons and mesenteric lymph node samples contained significantly reduced C2GnT activity compared to the level of activity in wild-type lysates (Fig. 7a). Furthermore, no significant C4GnT activity was detected in any tissue tested from C2GnT2-deficient mice, implying that C4GnT activity is produced exclusively by C2GnT2 (50, 69). In contrast, no significant decrease

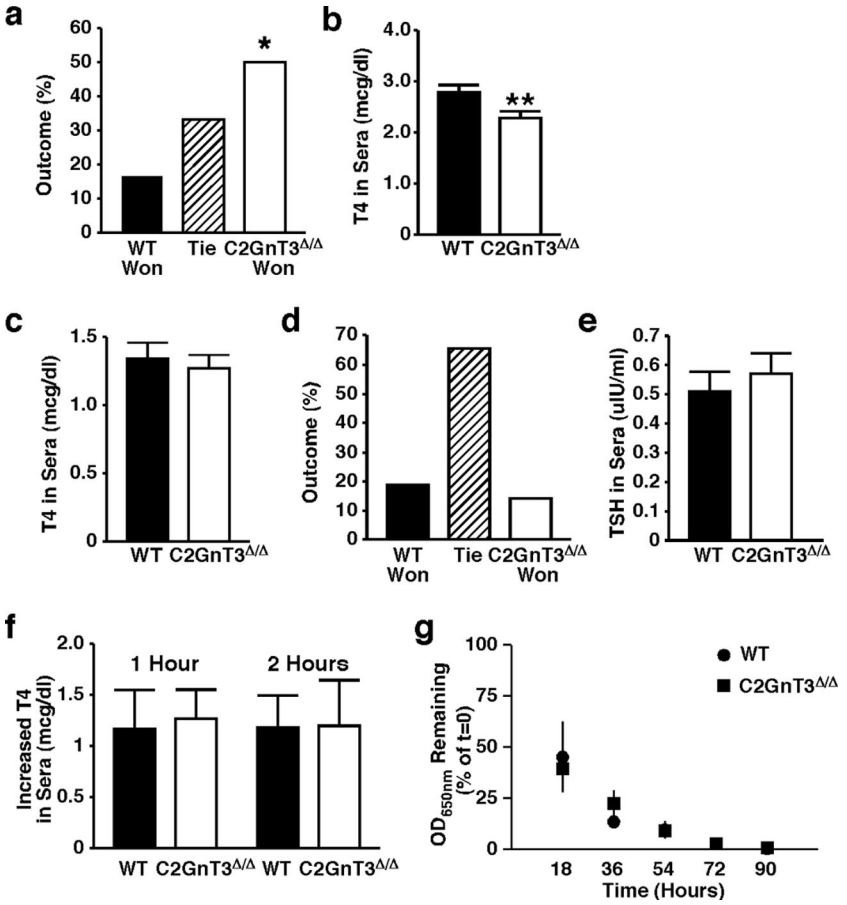

FIG. 6. Behavior and thyroid function in C2GnT3-deficient mice. (a) Results from the tube test for social dominance are graphed. The results shown are representative of three separate experiments. (b) The mean circulating T4 levels in wild-type and C2GnT3-deficient mice are graphed. (c) The mean circulating T4 levels in wild-type and C2GnT3-deficient mice after diet supplementation with 0.025% thyroid powder for 2 weeks are shown. (d) The outcome of social dominance assay performed with wild-type and C2GnT3-deficient mice treated with 0.025% thyroid powder supplemented chow is charted. (e) The mean circulating levels of the TSH in wild-type and C2GnT3-deficient mice are presented. (f) The average amount by which TRH stimulation increased T4 in circulation after 1 and 2 h in wild-type and C2GnT3-deficient mice is shown. (g) The mean relative amount of biotinylated T4 remaining at each time point is graphed. Error bars represent the SEM (*, $P < 0.05$; **, $P < 0.01$). WT, wild type.

in C2GnT activity was measured among various tissues analyzed from C2GnT3-deficient mice, despite the fact that the entire coding region of C2GnT3 was similarly deleted (Fig. 7b). Nevertheless, very little C2GnT activity was detected in tissues from mice deficient for all three C2GnTs (Fig. 7c).

O-glycan structures in C2GnT deficiency. O-glycan structures from C2GnT2 and C2GnT3 singly deficient mouse tissues were compared to wild-type samples using MS glycomic methodologies (25). The O-glycan structural changes reported herein have been selected among a larger number of alterations with a focus on the major defects observed. The full O-glycomes of each tissue remain to be established but will be reported elsewhere. Decreases in core 2 O-glycan structures, along with increases in various core 1 O-glycan structures, were clearly detected in C2GnT2-deficient stomach, colon, and small intestine samples (Fig. 8). In C2GnT2-deficient stomach and colon tissues, the increased abundance of core 1 structures included elongated core 1 branches, several of which bore polylactosamine. In contrast, in the small intestine nonelongated, sialylated core 1 O-glycan structures were increased. Furthermore, stomach and colon tissues from C2GnT2-deficient mice exhibited a decrease in I-branching. Surprisingly, elongated O-mannose structures were detected in the stomachs of C2GnT2-deficient mice but not in their wild-type counterparts. O-glycan structures from C2GnT2-deficient kidney samples were unaltered compared to wild-type kidney structures, a finding consistent with the relative expression of murine C2GnT2.

C2GnT3-deficient tissues contained O-glycan structural changes in the small intestine and thyroid/trachea samples, with a decreased abundance of some core 2 O-glycan structures relative to core 1 O-glycan structures in these tissues. No substantial changes in O-glycan structures were noted in the thymus, colon, kidney, or liver samples from C2GnT3-deficient mice (Fig. 8 and data not shown). These findings revealed that even in tissues with high relative expression of C2GnT3, loss of this glycosyltransferase did not lead to marked changes in O-glycan structures.

Tissues from T1/T2/T3 mice deficient in all three known C2GnTs lacked all detectable core 2 O-glycan structures among all tissues surveyed, including the colon, small intestine,

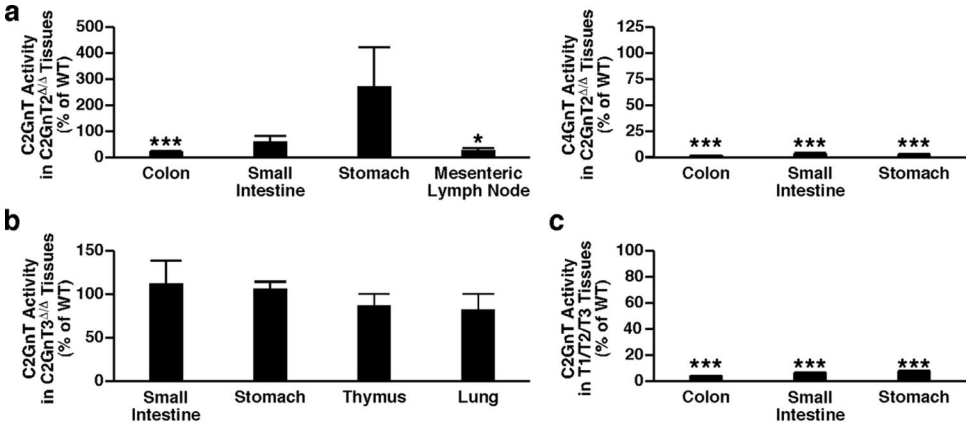

FIG. 7. Enzyme activity in tissue lysates from mice deficient for C2GnTs. (a) The relative C2GnT and C4GnT activities in tissue lysates from C2GnT2-deficient mice are graphed. (b and c) The C2GnT activity in tissue lysates from C2GnT3-deficient (b) and triply deficient (c) mice relative to the activity in wild-type control tissues is shown. Measurements shown represent means ± the SEM (*, $P < 0.05$; ***, $P < 0.001$).

stomach, and kidney (Fig. 8). These results indicate that no other glycosyltransferases appear capable of synthesizing core 2 O-glycans in vivo. Furthermore, small intestine, stomach, and colon samples from T1/T2/T3 mice had a further increase in elongated Core 1 O-glycans compared to tissues lacking a single C2GnT. Surprisingly, no O-glycan structures containing I-branches were detected in stomach and colon samples from T1/T2/T3 mice. There was also an unexpected increase in elongated O-mannose structures in the stomach of T1/T2/T3 mice, even in comparison to C2GnT2-deficient stomach samples.

DISCUSSION

The presence of three conserved genes encoding glycosyltransferases that can initiate the biosynthesis of Core 2 O-glycans suggests that each C2GnT may provide significant compensation for one another as afforded by this close though not complete overlap in enzymatic function. However, the different expression profiles of distinct C2GnTs among tissues and cell types further suggests that these closely related glycosyltransferases may have unique biological roles. By generating mice singly and multiply deficient in C2GnT activities, we have developed mammalian animal models for studying the structure and function of O glycosylation as controlled by C2GnT activity. Core 2 and perhaps core 4 O-glycans produced by C2GnT2 operate in establishing the epithelial mucosal barrier and reducing disease pathology after chemical induction of colitis. Alterations in humoral and mucosal immune system homeostasis were also detected and may be related to these findings. In contrast, C2GnT3 does not provide a role in the formation or maintenance of the mucosal barrier but instead alters behavioral phenotypes linked with T4 thyroxine abundance in circulation. Neither C2GnT2 nor C2GnT3 appear to function in the biosynthesis of selectin ligands, unlike findings in mice lacking C2GnT1 (14). Each C2GnT glycosyltransferase therefore has different biological roles among various physiological systems. Both expected and unexpected changes occurred in the repertoire of O-glycans detected among multiple tissues from mice deficient in C2GnT activity. These structural alterations of the glycome may aid in further resolving the mechanistic features of O-glycan biosynthesis and the etiology of these phenotypes.

Distinct and potential overlapping functions of C2GnTs. Neutrophilia in C2GnT3-deficient mice in the absence of a measured defect in selectin ligand, as determined by cytometry, is reminiscent of mice deficient for α(1,3)fucosyltransferase-IV (FucT-IV). In contrast, no hematological or selectin ligand biosynthetic defect was observed in C2GnT2 deficiency. Mice deficient for FucT-IV also exhibited a slight increase (20%) in neutrophils in circulation without measurable decreases in binding of selectin chimeras to neutrophils (23). Nevertheless, FucT-IV was shown to contribute to selectin ligand function in vivo, since FucT-IV deficiency increased selectin-dependent leukocyte rolling velocity in microvessels (65). It remains possible that C2GnT3 contributes to selectin ligand formation detectable by additional studies and approaches. Alternatively, C2GnT3 may modulate neutrophil abundance in circulation by altering myelopoiesis. Several cell adhesion molecules, including selectins and sialomucins, have been found to influence hematopoiesis, and altered glycosylation has been shown to increase neutrophil production (23, 53, 63). This may reflect altered binding between lectins and glycoproteins in the context of stem cell turnover and differentiation. Nevertheless, the degree of increase observed among circulating neutrophils per se in C2GnT3-deficient mice is unlikely to significantly alter physiology.

Decreased mucosal barrier function is associated with inflammatory bowel diseases (33, 55), including colitis. It is possible that the increased mucosal permeability and disease signs that occur with DSS treatment are related in C2GnT2-deficient mice. Moreover, the single C3GnT glycosyltransferase that generates core 3 O-glycans is also essential for mucosal barrier function and similarly decreases susceptibility to DSS-induced colitis (2). In C3GnT-deficient mice, these findings were attributed to a reduced abundance of Muc2, a mucin known to be necessary for protection from colitis (2, 60). In contrast, C2GnT2-deficient mice did not appear to have decreased expression of Muc2. Susceptibility to inflammatory bowel diseases is associated with factors other than altered mucin levels, including changes in commensal and pathogenic

Structural characteristics	Examples of structure	Changes relative to WT		
		C2GnT2$^{\Delta/\Delta}$	C2GnT3$^{\Delta/\Delta}$	T1/T2/T3
Stomach				
Core 2	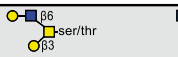	↓↓	=	ND
Elongated Core 1	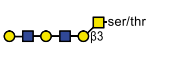	↑↑	=	↑↑↑
I- Branches		↓↓	=	ND
Elongated O-mannose		↑	=	↑↑↑
Colon				
Core 2		↓↓	=	ND
Elongated Core 1	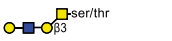	↑↑	=	↑↑↑
I- Branches	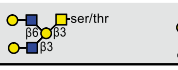	↓↓↓	=	ND
Small Intestine				
Core 2	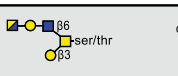	↓	↓↓	ND
Core 1 & Elongated Core 1		↑	↑↑	↑↑↑
Kidneys				
Core 2	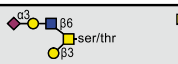	=	=	ND
Core 1 & Elongated Core 1	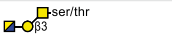	=	=	=
Thyroid / Trachea				
Core 2		NA	↓	NA
Core 1 & Elongated Core 1	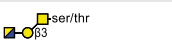	NA	↑	NA
Sd^a	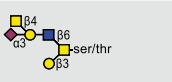	NA	↓	NA
Thymus				
Core 2	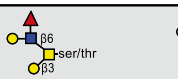	NA	=	NA
Core 1 & Elongated Core 1		NA	=	NA

FIG. 8. O-glycan structures in the presence or absence of C2GnTs. The structural changes described here are based on MALDI-TOF/TOF-MS and MS/MS data. WT, wild-type mice; C2GnT2$^{\Delta/\Delta}$, C2GnT2-deficient mice; C2GnT3$^{\Delta/\Delta}$, C2GnT3-deficient mice; T1/T2/T3, C2GnT triply deficient mice. NA, not analyzed, ND, not detected; =, no significant changes; ser, serine; thr, threonine. Upward arrows indicate increases, and downward arrows indicate decreases. The number of arrows is indicative of the magnitude of the change, with three arrows being the greatest (>75%) and one arrow being the smallest (<25%) percentage of change compared to the wild type. Linkages are assigned to the known biosynthetic pathways. Color symbols: yellow square, GalNAc; blue square, GlcNAc; half-blue/half-yellow square, GalNAc or GlcNAc; yellow circle, galactose; green circle, mannose; purple diamond, *N*-acetylneuraminic acid; white diamond, *N*-glycolylneuraminic acid; red triangle, fucose.

organisms, as well as altered immune system homeostasis (43, 66). In C2GnT2-deficient mice, the impaired humoral immune homeostasis exhibited by reduced serum IgG1, IgG2a, and IgG2b and mucosal IgA levels may indicate or contribute somehow to increased susceptibility to experimental colitis. Furthermore, since high relative expression of C2GnT2 is prominent among tissues with a high epithelial cell content, it is possible that the decrease in some immunoglobulin subtypes is due to a defect of the mucosal immune system. Perhaps the C2GnT2 and C3GnT glycosyltransferases collaborate to enforce the mucosal epithelial barrier.

Several mechanisms may explain the reduced T4 thyroxine abundance in C2GnT3-deficient mice. Alterations in the T4 negative-feedback loop could lead to decreased T4 abundance in the presence of normal TSH levels. Alternatively, it remains possible that decreased T4 half-life or T4 secretion in response to TSH stimulation in C2GnT3 deficiency occurs at levels below experimental detection. Additional studies that include analyses of T4 carrier proteins may further resolve this. From our findings, it remains possible that overly aggressive behavior linked to decreased T4 abundance may be among the first symptoms to develop in some cases of hypothyroidism.

Although mice singly deficient for C2GnT1, C2GnT2, or C2GnT3 exhibited distinct phenotypes, the presence of novel phenotypes in mice deficient for multiple C2GnTs, but not present in any of the singly deficient models, would reveal collaboration and compensation among these glycosyltransferases in physiologic processes. Preliminary data indicate that T1/T2/T3 mice are unique among the other lesser deficiency states with elevated levels of the liver enzyme alanine transaminase, implying changes in liver function apparent only in the absence of all three C2GnTs (unpublished observation). Defining the biological mechanisms of the phenotypes evoked by the loss of C2GnT activity will require additional resolution that is afforded by linking glycan structures to normal and pathological contexts.

Structural basis of O-glycan biosynthesis determined by C2GnT1, C2GnT2, and C2GnT3. The absence of any single C2GnT glycosyltransferase results in a reduction of core 2 O-glycan structures in one or more tissues in vivo. By comparison, the decrease in core 2 O-glycan structures in C2GnT3-deficient tissue samples was modest, and the C2GnT activity was not measurably decreased in these tissues. This suggests that C2GnT3 may have a relatively minor contribution to core 2 O-glycan biosynthesis in these tissue types in vivo. Core 2 O-glycan structures were totally absent from tissues lacking all three C2GnTs. Interestingly, tissue lysates from these triply deficient animals harbored a small amount of C2GnT enzymatic activity. This suggests the possibility that another unidentified glycosyltransferase may have a low level of C2GnT activity when assayed in vitro. Nevertheless, the absence of core 2 O-glycan structures in T1/T2/T3 mice indicates that no additional glycosyltransferases exist that can generate core 2 O-glycans in vivo as detected by our analyses.

C2GnT deficiency further altered the repertoire and abundance of O-glycan structures not directly generated by C2GnTs and produced by different biosynthetic pathways. The large decrease in the abundance of I-branching on O-glycan structures from stomach and colon tissues of mice lacking C2GnT2 suggests that in some tissues C2GnT2, and not IGnT, is the dominant I-branching glycosyltransferase in protein O glycosylation. The further loss of I-branching in stomach and colon samples from mice lacking all three C2GnTs implies that either C2GnT1 or C2GnT3 may also have I-branching activity in vivo. In this regard, C2GnT3 has been characterized with a low level of I-branching activity in vitro (51). The repertoire of core 1 O-glycans and O-mannosylated glycans were also altered among various tissues. The increase of core 1 O-glycan structures and their elongation in the absence of one or more C2GnTs was linked with the formation of polylactosamines that may alter lectin-dependent binding and physiology. This elaboration of core 1 O-glycans is probably not due to reduced competition for acceptor substrates in the Golgi apparatus, since the formation of the core 2 O-glycan branch does not decrease the efficiency of core 1 extension enzyme-β1,3-*N*-acetylglucosaminyltransferase (β3GnT3) (68). Alternate explanations include the possible elevation of β3GnT3 activity or perhaps an increase in the availability of the common UDP-GlcNAc donor substrate, which is also used in elaborating glycans that arise from protein O mannosylation (70, 72). Core 4 O-glycan structures, if present, exist below the level of detection in wild-type and C2GnT-deficient tissues; thus, it is not currently known whether the loss of C4GnT activity in C2GnT2 deficiency correlates with a reduction or absence of core 4 O-glycans in vivo.

Core 2 O-glycans have been associated with interactions among commensal and pathogenic bacteria and their hosts. Loss of C2GnT2 may alter the potential or frequency of gastrointestinal colonization by commensal or pathogenic bacteria. Recently, it has been shown that *Helicobacter pylori* and *Clostridium perfringens* express proteins that bind to core 2 O-glycans (5, 27), and preliminary data suggest that C2GnT3 may be required for T-cell responses to an intestinal challenge (H. Ziltener, unpublished data). These findings may relate to the phenotypes described here and suggest that challenging these animals with additional stimuli may provide mechanistic insights and perhaps further reveal novel biological roles for the core 2 O-glycans. The relatively mild impact of core 2 O-glycan deficiency in vivo may reflect compensation provided by the resulting induction of extended core 1 and O-mannosylated O-glycan structures. This has been observed in the formation of selectin ligands on extended Core 1 O-glycans in C2GnT1 deficiency (68). However, each of the three glycosyltransferases that contribute to C2GnT or C4GnT activity has a distinct function, and this begins to explain the conservation of three separate genes encoding glycosyltransferases that initiate the formation of core 2 O-glycans.

ACKNOWLEDGMENTS

We thank David Ditto for technical expertise with the hematological assays and Margo Streets and Trang Tran for technical expertise with the behavior assays. Jeffery Long assisted with the statistical analysis of the behavioral data.

This study was funded in part by a Mizutani Foundation for Glycoscience award (J.D.M.), a Veterans Affairs Merit Review Grant (S.B.H.), the University of California San Diego Digestive Disease Research Development Center (S.B.H), and National Institute of Health grants HL057345 (J.D.M.), HL78784 (J.D.M.), GMG2116 (J.D.M.), CA33000 (M.F.), and P01CA71932 (M.F. and J.D.M.). J.D.M. is supported by the Howard Hughes Medical Institute. This study was also funded in part by Biotechnology and Biological Sciences Research Council grant BBF0083091 (A.D.) and Public Health Service grant DK080506 (S.B.H.). M.N.I. is supported by University Science Malaysia, Ministry of Higher Education.

We declare that we have no competing financial interests.

REFERENCES

1. **Altschuler, Y., C. L. Kinlough, P. A. Poland, J. B. Bruns, G. Apodaca, O. A. Weisz, and R. P. Hughey.** 2000. Clathrin-mediated endocytosis of MUC1 is modulated by its glycosylation state. Mol. Biol. Cell **11:**819–831.
2. **An, G., B. Wei, B. Xia, J. M. McDaniel, T. Ju, R. D. Cummings, J. Braun, and L. Xia.** 2007. Increased susceptibility to colitis and colorectal tumors in mice lacking core 3-derived O-glycans. J. Exp. Med. **204:**1417–1429.
3. **Arkan, M. C., A. L. Hevener, F. R. Greten, S. Maeda, Z. W. Li, J. M. Long, A. Wynshaw-Boris, G. Poli, J. Olefsky, and M. Karin.** 2005. IKK0beta links inflammation to obesity-induced insulin resistance. Nat. Med. **11:**191–198.
4. **Aronson, L.** 1998. Animal behavior case of the month. Aggression directed toward other horses. J. Am. Vet. Med. Assoc. **213:**358–359.
5. **Ashida, H., R. Maki, Y. H. Ozawa, Tani, M. Kiyohara, M. Fujita, A. Imamura, H. Ishida, M. Kiso, and K. Yamamoto.** 2008. Characterization of two different endo-α-*N*-acetylgalactosaminidases from probiotic and pathogenic enterobacteria, *Bifidobacterium longum* and *Clostridium perfringens*. Glycobiology **18:**727–734.
6. **Baum, L. G.** 2002. Developing a taste for sweets. Immunity **16:**5–8.
7. **Bierhuizen, M. F., and M. Fukuda.** 1992. Expression cloning of a cDNA encoding UDP-GlcNAc:Gal β1-3-GalNAc-R (GlcNAc to GalNAc) β1-6GlcNAc transferase by gene transfer into CHO cells expressing polyoma large tumor antigen. Proc. Natl. Acad. Sci. USA **89:**9326–9330.
8. **Carlow, D. A., B. Ardman, and H. J. Ziltener.** 1999. A novel CD8 T cell-restricted CD45RB epitope shared by CD43 is differentially affected by glycosylation. J. Immunol. **163:**1441–1448.

9. **Cho, J. H.** 2008. The genetics and immunopathogenesis of inflammatory bowel disease. Nat. Rev. Immunol. **8:**458–466.
10. **Crawley, J. N.** 2007. What's wrong with my mouse? Behavioral phenotyping of transgenic and knockout mice. Wiley Interscience, New York, NY.
11. **Dahl, G. E., N. P. Evans, L. A. Thrun, and F. J. Karsch.** 1994. A central negative feedback action of thyroid hormones on thyrotropin-releasing hormone secretion. Endocrinology **135:**2392–2397.
12. **Dodman, N. H., P. A. Mertens, and L. P. Aronson.** 1995. Animal behavior case of the month: dogs were evaluated because of aggression. J. Am. Vet. Med. Assoc. **207:**1168–1171.
13. **deVos, T., and T. A. Dick.** 1991. A rapid method to determine the isotype and specificity of coproantibodies in mice infected with *Trichinella* or fed cholera toxin. J. Immunol. Methods **141:**285–288.
14. **Ellies, L. G., S. Tsuboi, B. Petryniak, J. B. Lowe, M. Fukuda, and J. D. Marth.** 1998. Core 2 oligosaccharide biosynthesis distinguishes between selectin ligands essential for leukocyte homing and inflammation. Immunity **9:**881–890.
15. **Fatjo, J., M. Amat, and X. Manteca.** 2003. Animal behavior case of the month: aggression in dogs. J. Am. Vet. Med. Assoc. **223:**623–626.
16. **Fliers, E., U. A. Unmehopa, and A. Alkemade.** 2006. Functional neuroanatomy of thyroid hormone feedback in the human hypothalamus and pituitary gland. Mol. Cell Endocrinol. **251:**1–8.
17. **Furuta, G. T., J. R. Turner, C. T. Taylor, R. M. Hershberg, K. Comerford, S. Narravula, D. K. Podolsky, and S. P. Colgan.** 2001. Hypoxia-inducible factor 1-dependent induction of intestinal trefoil factor protests barrier function during hypoxia. J. Exp. Med. **193:**1027–1034.
18. **Gauguet, J. M., S. D. Rosen, J. D. Marth, and U. H. von Andrian.** 2004. Core 2 branching β1,6-*N*-acetylglucosaminyltransferase and high endothelial cell *N*-acetylglucosamine-6-sulfotransferase exert differential control over B- and T-lymphocyte homing to peripheral lymph nodes. Blood **104:**4104–4112.
19. **Grewal, P. K., S. Uchiyama, D. Ditto, N. Varki, D. T. Le, V. Nizet, and J. D. Marth.** 2008. The Ashwell receptor mitigates the lethal coagulopathy of sepsis. Nat. Med. **14:**648–655.
20. **Hassan, H., C. A. Reis, E. P. Bennett, E. Mirgorodskaya, P. Roepstorff, M. A. Hollingsworth, J. Burchell, J. Taylor-Papadimitriou, and H. Clausen.** 2000. The lectin domain of UDP-*N*-acetyl-D-galactosamine: polypeptide *N*-acetylgalactosaminyltransferase-T4 directs its glycopeptide specificities. J. Biol. Chem. **275:**38197–38205.
21. **Hiraoka, N., H. Kawashima, B. Petryniak, J. Nakayama, J. Mitoma, J. D. Marth, J. B. Lowe, and M. Fukuda.** 2004. Core 2 branching β1,6-*N*-acetylglucosaminyltransferase and high endothelial venule-restricted sulfotransferase collaboratively control lymphocyte homing. J. Biol. Chem. **279:**3058–3067.
22. **Ho, S. B., L. A. Dvorak, R. E. Moor, A. C. Jacobson, M. R. Frey, J. Corredor, D. B. Polk, and L. L. Shekels.** 2006. Cysteine-rich domains of Muc3 intestinal mucin promote cell migration, inhibit apoptosis, and accelerate wound healing. Gastroenterology **131:**1501–1517.
23. **Homeister, J. W., A. D. Thall, B. Petryniak, P. Maly, C. E. Rogers, P. L. Smith, R. J. Kelly, K. M. Gersten, S. W. Askari, G. Cheng, G. Smithson, R. M. Marks, A. K. Misra, O. Hindsgaul, U. H. von Andrian, and J. B. Lowe.** 2001. The α(1,3)fucosyltransferases FucT-IV and FucT-VII exert collaborative control over selectin-dependent leukocyte recruitment and lymphocyte homing. Immunity **15:**115–126.
24. **Iwai, T., N. Inaba, A. Naundorf, Y. Zhang, M. Gotoh, H. Iwasaki, T. Kudo, A. Togayachi, Y. Ishizuka, H. Nakanishi, and H. Narimatsu.** 2002. Molecular cloning and characterization of a novel UDP-GlcNAc:GalNAc-peptide β1,3-*N*-acetylglucosaminyltransferase (β3Gn-T6), an enzyme synthesizing the core 3 structure of O-glycans. J. Biol. Chem. **277:**12802–12809.
25. **Jang-Lee, J., S. J. North, M. Sutton-Smith, D. Goldberg, M. Panico, H. Morris, S. Haslam, and A. Dell.** 2006. Glycomic profiling of cells and tissues by mass spectrometry: fingerprinting and sequencing methodologies. Methods Enzymol. **415:**59–86.
26. **Ju, T., K. Brewer, A. D'Souza, R. D. Cummings, and W. M. Canfield.** 2002. Cloning and expression of human core 1 β1,3-galactosyltransferase. J. Biol. Chem. **277:**178–186.
27. **Kawakubo, Y. M., Ito, Y. Okimura, M. Kobayashi, K. Sakura, S. Kasama, M. N. Fukuda, M. Fukuda, T. Katsuyama, and J. Nakayama.** 2004. Natural antibiotic function of a human gastric mucin against *Helicobacter pylori* infection. Science **305:**1003–1006.
28. **Long, J. M., P. LaPorte, S. Merscher, B. Funke, B. Saint-Jore, A. Puech, R. Kucherlapati, B. E. Morrow, A. I. Skoultchi, and A. Wynshaw-Boris.** 2006. Behavior of mice with mutations in the conserved region deleted in velocardiofacial/DiGeorge syndrome. Neurogenetics **7:**247–257.
29. **Long, J. M., P. LaPorte, R. Paylor, and A. Wynshaw-Boris.** 2004. Expanded characterization of the social interaction abnormalities in mice lacking *Dvl1*. Genes Brain Behav. **3:**51–62.
30. **Lowe, J. B.** 2001. Glycosylation, immunity, and autoimmunity. Cell **104:**809–812.
31. **Lowe, J. B., and J. D. Marth.** 2003. A genetic approach to mammalian glycan function. Annu. Rev. Biochem. **72:**643–691.
32. **Magnet, A. D., and M. Fukuda.** 1997. Expression of the large I antigen forming β-1,6-*N*-acetylglucosaminyltransferase in various tissues of adult mice. Glycobiology **7:**285–295.
33. **Mankertz, J., and J. D. Schulzke.** 2007. Altered permeability in inflammatory bowel disease: pathophysiology and clinical implications. Curr. Opin. Gasteroenterol. **23:**379–383.
34. **Marians, R. C., L. Ng, H. C. Blair, P. Unger, P. N. Graves, and T. F. Davies.** 2002. Defining thyrotropin-dependent and -independent steps of thyroid hormone synthesis by using thyrotropin receptor-null mice. Proc. Natl. Acad. Sci. USA **99:**15776–15781.
35. **Marth., J. D. and P. K. Grewal.** 2008. Mammalian glycosylation in immunity. Nat. Rev. Immunol. **8:**874–887.
36. **Merzaban, J. S., J. Zuccolo, S. Y. Corbel, M. J. Williams, and H. J. Ziltener.** 2005. An alternate Core 2β1,6-*N*-acetylglucosaminyltransferase selectively contributes to P-selectin ligand formation in activated CD8 T cells. J. Immunol. **174:**4051–4059.
37. **Murthy, A. K., C. N. Dubose, J. A. Banas, J. J. Coalson, and B. P. Arulanandam.** 2006. Contribution of polymeric immunoglobulin receptor to regulation of intestinal inflammation in dextran sulfate sodium-induced colitis. Gastroenterology **26:**1372–1380.
38. **Murthy, S. N., H. S. Cooper, H. Shim, R. S. Shah, S. A. Ibrahim, and D. J. Sedergran.** 1993. Treatment of dextran sulfate sodium-induced murine colitis by intracolonic cyclosporine. Dig. Dis. Sci. **38:**1722–1734.
39. **Nagy, A., J. Rossant, R. Nagy, W. Abramow-Newerly, and J. C. Roder.** 1993. Derivation of completely cell culture-derived mice from early-passage embryonic stem cells. Proc. Natl. Acad. Sci. USA **90:**8424–8428.
40. **Okayasu, I., S. Hatakeyama, M. Yamada, T. Ohkusa, Y. Inagaki, and R. Nakaya.** 1990. A novel method in the induction of reliable experimental acute and chronic ulcerative colitis in mice. Gastroenterology **98:**694–702.
41. **Oliveira, K. J., T. M. Ortiga-Carvalho, A. Cabanelas, M. A. Veiga, K. Aoki, H. Ohki-Hamazaki, K. Wada, E. Wada, and C. C. Pazos-Moura.** 2006. Disruption of neuromedin B receptor gene results in dysregulation of the pituitary-thyroid axis. J. Mol. Endocrinol. **36:**73–80.
42. **Perez-Vilar, J., and R. L. Hill.** 1999. The structure and assembly of secreted mucins. J. Biol. Chem. **274:**31751–31754.
43. **Peterson, D. A., D. N. Frank, N. R. Pace, and J. I. Gordon.** 2008. Metagenomic approaches for defining the pathogenesis of inflammatory bowel disease. Cell Host Microbe **3:**417–427.
44. **Raman, J., T. A. Fritz, T. A. Gerken, O. Jamison, D. Live, M. Liu, and L. A. Tabak.** 2008. The catalytic and lectin domains of UDP-GalNAc:polypeptide α-*N*-acetylgalactosaminyltransferasae function in concert to direct glycosylation site selection. J. Biol. Chem. **283:**22942–22951.
45. **Rosen, S. D.** 2004. Ligands for L-selectin: homing, inflammation, and beyond. Annu. Rev. Immunol. **22:**129–156.
46. **Rossi, F. M. V., S. Y. Corbel, J. S. Merzaban, D. A. Carlow, K. Gossens, J. Duenas, L. So, L. Yi, and H. J. Ziltener.** 2005. Recruitment of adult thymic progenitors is regulated by P-selectin and its ligand PSGL-1. Nat. Immunol. **6:**626–634.
47. **Satsangi, J., M. Parkes, E. Louis, L. Hashimoto, N. Kato, K. Welsh, J. D. Terwilliger, G. M. Lathrop, J. I. Bell, and D. P. Jewell.** 1996. Two stage genome-wide search in inflammatory bowel disease provides evidence for susceptibility loci on chromosomes 3, 7, and 12. Nat. Genet. **14:**199–202.
48. **Schachter, H.** 2000. The joys of HexNAc: the synthesis and function of N- and O-glycan branches. Glycoconj. J. **17:**465–483.
49. **Schachter, H., and I. Brockhausen.** 1989. The biosynthesis of branched O-glycans. Symp. Soc. Exp. Biol. **43:**1–26.
50. **Schwientek, T., M. Nomoto, S. B. Levery, G. Merkx, A. G. van Kessel, E. P. Bennett, M. A. Hollingsworth, and H. Clausen.** 1999. Control of O-glycan branch formation: molecular cloning of human cDNA encoding a novel β1,6-*N*-acetylglucosaminyltransferase forming core 2 and core 4. J. Biol. Chem. **274:**4504–4512.
51. **Schwientek, T., J. C. Yeh, S. B. Levery, B. Keck, G. Merkx, A. G. van Kessel, M. Fukuda, and H. Clausen.** 2000. Control of O-glycan branch formation: molecular cloning and characterization of a novel thymus-associated Core 2 β1,6-N-acteylglucosaminyltransferase. J. Biol. Chem. **275:**11106–11113.
52. **Shafi, R., S. P. Iyer, L. G. Ellies, N. O'Donnell, K. W. Marek, D. Chui, G. W. Hart, and J. D. Marth.** 2000. The O-GlcNAc transferase gene resides on the X chromosome and is essential for embryonic stem cell viability and mouse ontogeny. Proc. Natl. Acad. Sci. USA **97:**5735–5739.
53. **Simmons, P. J., J. Levesque, and D. N. Haylock.** 2001. Mucin-like molecules as modulators of the survival and proliferation of primitive hematopoietic cells. Ann. N. Y. Acad. Sci. **938:**196–207.
54. **Stanley, P.** 2007. Regulation of Notch signaling by glycosylation. Curr. Opin. Struct. Biol. **17:**530–535.
55. **Stein, J., J. Ries, and K. B. Barrett.** 1998. Disruption of intestinal barrier function associated with experimental colitis: possible role of mast cells. Am. J. Physiol. **274:**G203–G209.
56. **Sutton-Smith, M., H. R. Morris, and A. Dell.** 2000. A rapid mass spectrometric strategy suitable for the investigation of glycan alterations in knockout mice. Tetrahedron Asymmetry **11:**363–369.
57. **Tarp, M. A., and H. Clausen.** 2008. Mucin-type O glycosylation and its potential use in drug and vaccine development. Biochim. Biophys. Acta **1780:**546–563.

58. **Ten Hagen, K. G., T. A. Fritz, and L. A. Tabak.** 2003. All in the family: the UDP-GalNAc:polypeptide *N*-acetylgalactosaminyltransferases. Glycobiology **13:**1R–16R.
59. **Tenno, M., K. Ohtsubo, F. K. Hagen, D. Ditto, A. Zarbock, P. Schaerli, U. H. von Andrian, K. Ley, D. Le, L. A. Tabak, and J. D. Marth.** 2007. Initiation of protein O glycosylation by polypeptide GalNAcT-1 in vascular biology and humoral immunity. Mol. Cell. Biol. **27:**8783–8796.
60. **van der Sluis, M., B. A. E. de Koning, A. C. J. M. de Bruijn, A. Velcich, J. P. P. Meijerink, J. B. van Goudoever, H. A. Buller, and A. W. C. Einerhand.** 2006. Muc2-deficient mice spontaneously develop colitis, indicating that Muc2 is critical for colonic protection. Gastroenterology **131:**117–129.
61. **Varki, A.** 2006. Nothing in glycobiology makes sense, except in the light of evolution. Cell **126:**841–845.
62. **Venero, C., A. Guadano-Ferraz, A. I. Herrero, K. Nordstrom, J. Manzano, G. M. de Escobar, J. Bernal, and B. Vennstrom.** 2005. Anxiety, memory impairment, and locomotor dysfunction caused by a mutant thyroid hormone receptor α1 can be ameliorated by T3 treatment. Genes Dev. **19:**2152–2163.
63. **Verfaillie, C. M.** 1998. Adhesion receptors as regulators of the hematopoietic process. Blood **92:**2609–2612.
64. **Wang, H., R. Tang, W. Zhang, K. Amirikian, Z. Geng, J. Geng, R. P. Hebbel, L. Xia, J. D. Marth, M. Fukuda, S. Katoh, and Y. Huo.** 2009 Core 2 1-6-*N*-glucosaminyltransferase-I is crucial for the formation of atherosclerotic lesions in apolipoprotein E-deficient mice. Arterioscler. Thromb. Vasc. Biol. **29:**180–187.
65. **Weninger, W., L. H. Ulfman, G. Cheng, N. Souchkova, E. J. Quackenbush, J. B. Lowe, and U. H. von Andrian.** 2000. Specialized contributions by α(1,3)-fucosyltransferase-IV and FucT-VII during leukocyte rolling in dermal microvessels. Immunity **12:**665–676.
66. **Xavier, R. J., and D. K. Podolsky.** 2007. Unraveling the pathogenesis of inflammatory bowel disease. Nature **448:**427–434.
67. **Yamada, M., Y. Saga, N. Shibusawa, J. Hirato, M. Murakami, T. Iwasaki, K. Hashimoto, T. Satoh, K. Wakabayashi, M. M. Taketo, and M. Mori.** 1997. Tertiary hypothyroidism and hyperglycemia in mice with targeted disruption of the thyrotropin-releasing hormone gene. Proc. Natl. Acad. Sci. USA **94:**10862–10867.
68. **Yeh, J. C., N. Hiraoka, B. Petryniak, J. Nakayama, L. G. Ellies, D. Rabuka, O. Hindsgaul, J. D. Marth, J. B. Lowe, and M. Fukuda.** 2001. Novel sulfated lymphocyte homing receptors and their control by a Core1 extension β1,3,-*N*-acetylglucosaminyltransferase. Cell **105:**957–969.
69. **Yeh, J. C., E. Ong, and M. Fukuda.** 1999. Molecular cloning and expression of a novel β-1,6-*N*-acetylglucosaminyltransferase that forms Core 2, Core 4, and I branches. J. Biol. Chem. **274:**3215–3221.
70. **Yoshida, A., K. Kobayashi, H. Manya, K. Taniguchi, H. Kano, M. Mizuno, T. Inazu, H. Mitsuhashi, S. Takahashi, M. Takeuchi, R. Herrmann, V. Straub, B. Talim, T. Voit, H. Topaloglu, T. Toda, and T. Endo.** 2001. Muscular dystrophy and neuronal migration disorder caused by mutations in a glycosyltransferase, POMGnT1. Dev. Cell **1:**717–724.
71. **Zachara, N. E., and G. W. Hart.** 2006. Cell signaling, the essential role of O-GlcNAc. Biochim. Biophys. Acta **1761:**599–617.
72. **Zhang, W., D. Betel, and H. Schachter.** 2002. Cloning and expression of a novel UDP-GlcNAc:α-3-D-mannoside β1,2-*N*-acetylglucosaminyltransferase I. Biochem. J. **361:**153–162.